Structural, optical and electrical properties of the fabricated Schottky diodes based on ZnO, Ce and Sm doped ZnO films prepared via wet chemical technique

MAM Ahmed[*a,b], WE Meyer[a], JM Nel[a]

[a]*Department of Physics, University of Pretoria, Private Bag X20, 0028 Hatfield, South Africa*
[b]*Department of Physics, Faculty of Education, University of Khartoum, P.O Box 321, 11115, Omdurman, Sudan*

Abstract

In this study, we fabricated Schottky diode devices on ZnO, Sm and Ce doped and co-doped ZnO thin films grown by the sol-gel spin coating. The structural and optical properties of the sol-gel films are studied, and the electrical characteristics of the Schottky diodes are investigated. The crystalline structure and surface morphology were studied using x-ray diffraction and scanning electron microscopy, respectively. Photoluminescence spectroscopy of all films measured at room temperature showed that the UV emission peak was composed of two peaks located at 388 and 405 nm and no visible light emission was detected. UV-vis study revealed that the optical band gap of ZnO decreased after doping. Room temperature *I-V* characterization revealed a rectification behaviour of all samples. The Schottky diodes fabricated on (Sm and Ce) co-doped ZnO manifest device properties with good rectification (six orders of magnitude), low ideality factor (1.62) and barrier height of 0.82 eV.

Keywords: ZnO; Sol gel; Structural properties; Optical properties; Electrical properties.

1. Introduction

Wide band gap semiconductors are of great interest because of their optoelectronic applications. These materials are used in the fabrication of devices such as light emitting diodes (LEDs) [1], dye-synthesized solar cells [2], thin film photovoltaic cells [3] and Schottky diodes [4, 5]. Zinc oxide (ZnO) as wide band gap semiconductor has been studied extensively over the past decade. ZnO, having an energy gap of 3.37 eV, is a very promising candidate in the electronic applications due to its low cost, low temperature growth [6], easy formation of nanostructures, its resistance to radiation damage [7], non-toxicity, the abundance of Zn compared to In and Ga [8]. In addition, ZnO has a large exciton binding energy of 60 meV at room temperature which enhances the light emission [9]. Moreover, ZnO has been used in a wide range of electronic devices such LEDs [10], gas sensors [11, 12], laser diodes [13], UV photodetectors [14] and Schottky diode devices [15].

The structural, optical and electrical properties of ZnO can be altered by doping with some cations. Transition metals have been used as dopants, and the resulting properties of the ZnO have been studied [16, 17, 18]. Recently, rare earth (RE) have been used as dopants for ZnO due to their high fluorescence efficiencies and the availability of the 4f orbital which results in interesting optical and electrical properties [19]. Numerous reports are available on RE doping of ZnO for example, Er [20], Ce [21], Yb, La [22] and Sm [23]. These REs can effectively modify the optical and electrical properties, making them good candidates for phosphors, multicoloured LEDs and Schottky diodes devices. Among these RE elements, Sm and Ce doped ZnO have been studied extensively due to their optical and electrical properties [24, 25]. Recently, both Sm and Ce doped ZnO nanorods have produced good Schottky diodes device with indium tin oxide and palladium as ohmic and rectifying contacts, respectively [4, 26]. In this study, we fabricate Schottky diodes based on the Sm, Ce doped and co-doped ZnO thin films and study their structural, optical and electrical properties.

There have been a variety of techniques used to prepare ZnO thin films. These include molecular beam epitaxy [27], metalorganic chemical vapour deposition [28], spray pyrolysis [29], pulsed laser deposition [30] and sol-gel spin

---

coating [31]. The sol-gel spin coating was adapted to synthesize the samples on the glass and n-Si substrates. The advantages of using the sol-gel techniques over the methods mentioned above are low cost, simplicity and versatility of the experimental setup, homogeneity, large area production and lower temperature crystallization. The films deposited on microscope glass slide substrates were used for the characterization of structural and optical properties, while films deposited on the n-Si substrates used for device fabrication and electrical characterization. There are some reports available on ZnO Schottky diodes with added Sm and Ce, however, to the best of our knowledge none has studied or reported on the fabrication of Schottky diodes based on Sm and Ce co-doped ZnO thin films. In this study, the structural, optical and electrical properties of the fabricated ZnO Schottky diodes with added Sm and Ce are studied in detail. The fabricated diodes exhibited rectification with six orders of magnitude difference between forward and reverse with ideality factor of 1.62 and barrier height of 0.82 eV.

2. Experimental methods

2.1. Materials

In these experiments the following raw materials were used as received without any further purification: zinc acetate dihydrate (98%, Merck), propan-2-ol (99.95%, Merck), monoethanolamine (MEA) (98%, Merck), samarium nitrate hexahydrate (99.9%, Sigma Aldrich) and cerium nitrate hexahydrate (99.999%, Sigma Aldrich).

2.2. Preparation of undoped, Sm and Ce doped and co-doped ZnO thin films

Zinc oxide sol-gel solution was prepared by dissolving zinc acetate dihydrate in propan-2-ol (60 ml) which was stirred at 500 rpm and 60 °C for 1 h. Thereafter, MEA with a molar ratio to zinc acetate of (1:1) was added drop-wise as a stabilizer to the solution while continuously stirring for 1 h under the same conditions. The sol-gel solutions for the doped material were prepared by adding 2 at% of samarium nitrate or/and cerium nitrate to the above solution using the same procedures used to prepare ZnO sol-gel. The clear, transparent solutions were then aged for 72 h before use, to increase their viscosity. Prior to the deposition, glass substrates were cleaned with deionized water, ethanol, and acetone, in this order for 15 min each using an ultrasonic bath, and finally blown dry with nitrogen gas. Si substrates were cleaned with trichloroethylene, isopropanol, methanol and deionized water sequentially using an ultrasonic bath for 5 min each [32]. Finally, Si substrates were etched by HF before evaporating the ohmic contact. Prepared sol-gels were then spin coated on pre-cleaned substrates (glass and Si) 4 layers at 3000 rpm for 30 s, then drying in an oven preheated at 130°C for 5 min. This process was repeated until the desired thickness was obtained. Finally, coated substrates were dried at 150 °C for 15 min to remove any remaining organic residual. Before subjecting the samples to characterization, those deposited on glass substrates were annealed at 500 °C in air (1 h), while samples deposited on n-Si substrates were annealed at the same temperature under a flow of Ar gas (30 min). A schematic diagram demonstrating samples preparation procedures is shown in Fig. 1 (a). Samples labelled as 1, 2, 3 and 4 for undoped ZnO, Sm-doped ZnO, Ce-doped ZnO and (Sm, Ce) co-doped ZnO thin films, respectively.

2.3. Deposition of the ohmic and Schottky contacts

For the fabrication of the contacts, n-type Si (111) substrate (ρ is 1.4 - 1.8 Ω.cm and carrier concentrations of 2.26 $\times 10^{15}$ cm^{-3}) was used in this study. 150 nm of Au-Sb alloy contact was evaporated resistively onto the back side of the Si substrate which served as ohmic contacts as depicted in Fig. 1 (b). The evaporated AuSb layer was then annealed at 375 °C for 10 min under flowing of Ar gas before spin coating the sol-gel on the front surface. For the Schottky contacts, 100 nm thick circular (0.8 mm diameter) Pd contacts were evaporated resistively on the thin films through a mechanical shadow mask. The Au-Sb and Pd contacts were deposited in a vacuum chamber at a pressure of 3.5×10^{-6} mbar and deposition rate of 0.1 nm/s.

3. Characterization

The as-synthesized pure ZnO, Sm and Ce doped ZnO and co-doped ZnO thin films were characterized regarding their structure, morphology and elemental analysis with X-ray diffraction (XRD) using Bruker D8 ADVANCE (λ = 1.5406 nm) and Zeiss Ultra Plus Field Emission Scanning Electron Microscopy (FESEM) integrated with energy dispersive X-ray spectroscopy (EDX). Photoluminescence of the as-synthesized samples in the range 350 - 650 nm
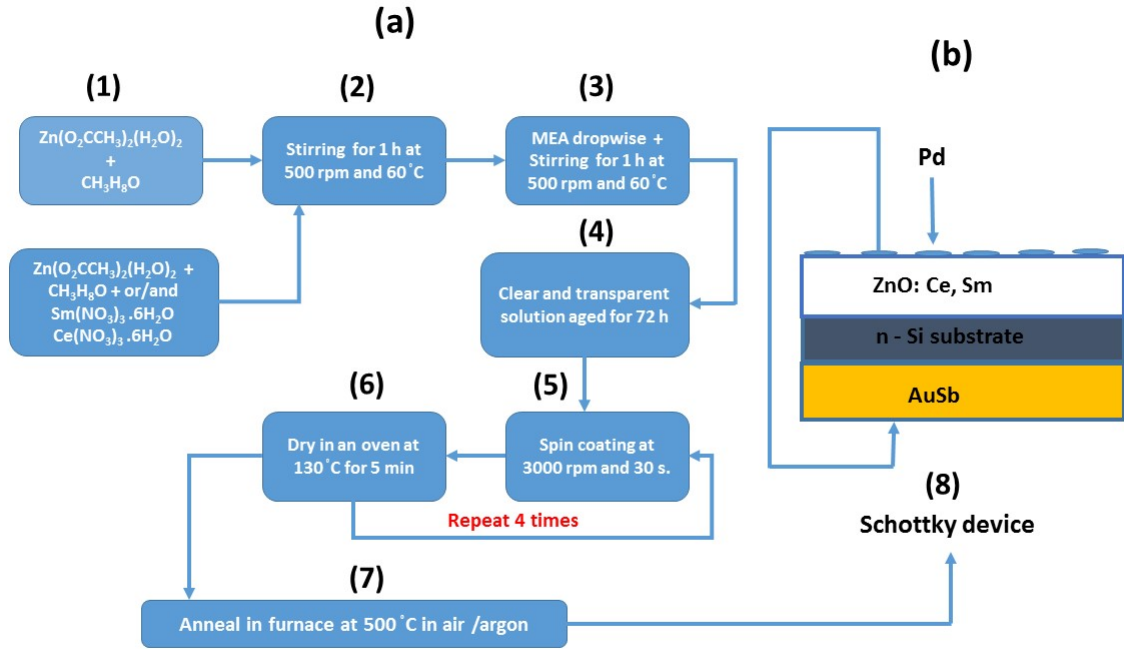
Figure 1: (Color online) (a) Schematic diagram of the preparation procedures for undoped ZnO and (Sm, Ce) doped and co-doped ZnO thin films. (b) On which the AuSb ohmic contacts and Pd Schottky contacts are deposited to produce the Schottky device.

was studied using a Cary Eclipse fluorescence spectrometer. A Varian Cary 100 UV-vis spectrometer was used for measuring the optical transmittance of the as-synthesized samples at room temperature. Before taking the UV-vis measurements, the background was taken using a pre-cleaned blank glass substrate. Finally, electrical analysis on Schottky diodes fabricated on pure, Sm and Ce doped ZnO and co-doped ZnO thin films were performed at room temperature using HP 4140B pA meter/DC voltage source.

4. Results and discussion

4.1. Structural and morphological results

Fig. 2(A) shows the XRD pattern of undoped, Sm and Ce doped and co-doped ZnO thin films measured at room temperature. The peaks observed in the XRD spectrum assigned to the wurtzite ZnO structure with no other peaks related to impurities or Sm and Ce phases. The XRD patterns obtained for all the thin films are similar to those reported earlier [24, 33, 34]. As evidenced in Fig. 2, the as-synthesized samples were polycrystalline with the main peaks (100), (002) and (101). The absence of Sm, Ce, Sm_2O_3, CeO_2 and Ce_2O_3 peaks in the XRD spectrum indicates that the Sm^{+3} or/and Ce^{+3}/Ce^{+4} substituted the Zn^{+2} and incorporated successfully into the ZnO lattice. This also emphasized that, the concentrations of the dopants below the solubility limit. The sections of XRD patterns in Fig. 2 (B) showed a shift in the peak position of the plane (100), (002) and (101) toward lower 2 theta values upon doping the ZnO with the shift being more pronounced in the case of Sm-doped samples. However, for the Ce and Sm co-doping, the shift was toward higher 2 theta values. This shift could be due to the larger ionic radius of Sm^{+3}, Ce^{+3} and Ce^{+4} (0.94, 1.03 and 0.92 Å) than that of Zn^{+2} (0.74 Å). It also observed that the peak intensities of the (100), (002) and (101) decreased. This could be attributed to the degradation of the crystalline quality of the samples.

The crystallographic properties of all the thin films are summarized in Table 1. The calculated lattice constants for pure ZnO is in good agreement with JCPDF # 751526. The lattice parameters for Sm-doped ZnO thin films at

3
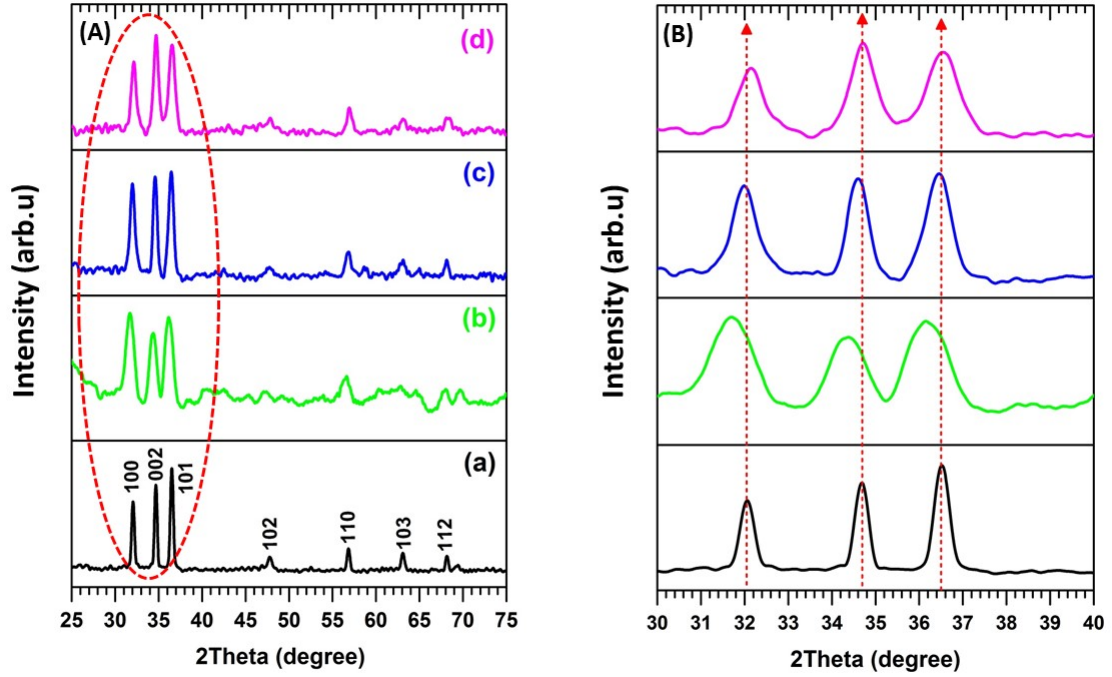
Figure 2: (A) The XRD pattern of samples annealed at 500 °C: (a) undoped, (b) Sm-doped, (c) Ce-doped and (d) Sm and Ce co-doped ZnO thin films. (B) Enlargement of (100), (002) and (101) peaks.

Table 1: Lattice parameters, peak position (2θ), FWHM, particle size (D) and unit cell volume (V) of as-synthesized annealed at 500 °C.

Samples	Lattice (Å)		2θ (degree)			FWHM (degree)			D (nm)			V
#	a	c	(100)	(002)	(101)	(100)	(002)	(101)	(100)	(002)	(101)	(Å^3)
1	3.212	5.166	32.06	34.68	36.51	0.370	0.351	0.398	22.38	22.57	20.80	46.35
2	3.248	5.206	31.69	34.36	36.18	1.095	1.003	1.158	7.25	7.92	6.86	47.56
3	3.226	5.178	31.99	34.59	36.43	0.646	0.550	0.687	12.37	14.44	11.55	46.66
4	3.311	5.163	32.14	34.71	36.53	0.667	0.681	0.822	11.95	11.75	9.65	49.02

2 at% are similar to values previously reported [26]. As can be seen from Table 1, the lattice parameter increased for the doped samples compared to undoped ZnO. The change in the lattice parameters and the position of the main peaks (i.e. (100), (002) and (101)) are more pronounced in the case of Sm and Ce co-doped ZnO thin films. This could be due to the distortion in the ZnO lattice due to the larger ionic radius of the dopants. The full widths at half maximum (FWHM) were found to increase when dopants introduced. The average crystallite size D was calculated using Debye-Sherer's formula [35] and was found to be smaller for the doped samples compared to the undoped ZnO. Similar results were previously observed by Kulandaisamy *et al.* and Yousefi and co-authors [24, 36]. Furthermore, the volume of the unit cell (V) [26] was found to increase on doping. Fig. 3 shows the SEM images of the samples after annealing at 500 °C. The SEM images show that uniform films obtained with particle sizes ranging from 9.65 to 22.57 nm. The particle size of the Ce and Sm co-doped ZnO films became larger as shown in Fig. 3. EDX spectra of as-synthesized samples show that beside the Zn and O, Sm and Ce were detectable in the doped thin films. These results combined with XRD spectra support the conclusion that the Sm and Ce have incorporated into the ZnO lattice.
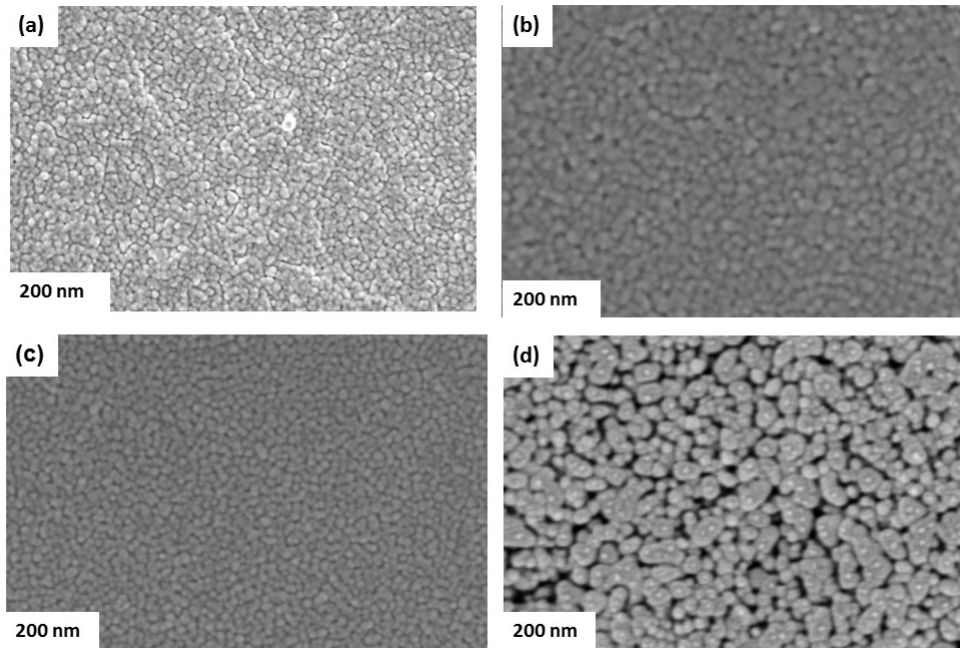
Figure 3: SEM images: (a) undoped, (b) Sm-doped, (c) Ce-doped and (d) Sm and Ce co-doped ZnO thin films.

4.2. Photoluminescence

Fig. 4 shows the photoluminescence (PL) spectra of undoped, Sm and Ce doped and co-doped ZnO thin films, respectively, measured at room temperature using an excitation wavelength of 342 nm. The as-synthesised samples annealed at 500 °C in air for 1 h show two characteristic emission peaks in PL spectra namely UV and weak blue emission located at about 470 nm, as depicted in Fig. 4. The UV emission, also known as a near band edge emission, originates from the free exciton recombination (i.e. recombination between electron and holes) of ZnO [37, 38]. The UV emission consists of two peaks located at 388 nm and 405 nm. The emission line determined at 405 nm is due to the defect emission [39]. As seen in Fig. 4, the intensity of the 405 peak increased and became sharper when the Sm dopant introduced compared to other samples. The presence of a sharp UV peak indicates that Sm improved the quality of the samples. The blue color emission at about 470 nm is has been previously attributed to zinc interstitial defects in ZnO or quantum confinement [40, 41]. Interestingly, the PL spectra of the annealed samples presented in Fig. 4 did not show any visible (deep level) emission which usually seen in the PL spectra of ZnO. The disappearance of the yellow-green emission indicates that the annealing removed the defects from the samples and improved the crystalline quality. Similar behaviour was also reported for sol-gel Al-doped ZnO thin films [42].

4.3. UV-vis transmittance spectroscopy

Fig. 5 shows the UV-vis transmittance spectra of pure ZnO, Sm and Ce doped ZnO and co-doped ZnO thin films measured at room temperature in the range 200 - 800 nm. The transmittance increased when doping with Sm and Ce compared to undoped ZnO,and however, for the co-doped samples, transmittance decreased from 75 % to 62 %. This can be explained concerning the sample's surface roughness: Atomic force microscopy analysis (not shown here) found surface roughness for undoped ZnO, Sm and Ce doped and co-doped ZnO films to be 28, 18, 19 and 34 nm, respectively. The co-doped sample had the most significant surface roughness and therefore, highest scattering and lowest transmittance. This optical scattering may be caused by the different particle sizes formed at the surface during the growth as well as the surface roughness. As seen from Fig. 5, the Sm and Ce doped ZnO samples have a higher transmittance and lower surface roughness with respect to undoped ZnO. Similar results were reported for Ce and Ce_2O doped ZnO films grown by dip coating and metal organic chemical vapour deposition, respectively [36, 43].
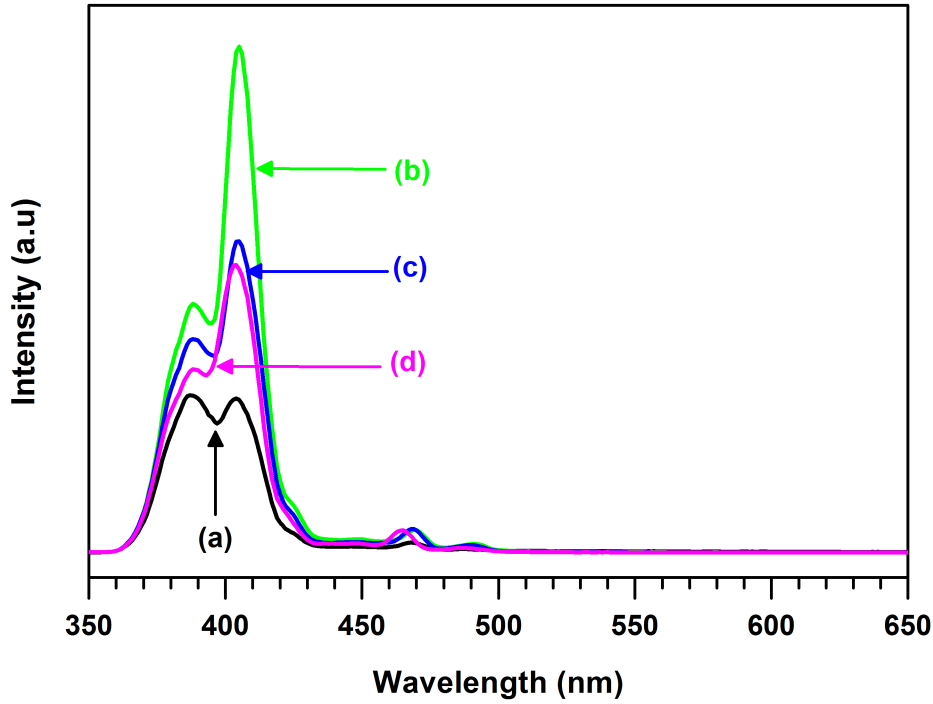
Figure 4: (Color online) Photoluminescence spectra of samples annealed at 500 ° C in air for 1 h: (a) undoped, (b) Sm-doped, (c) Ce-doped and (d) Sm and Ce co-doped ZnO thin films.

According to the optical absorption theory of a direct band gap semiconductor, the optical band gap (E_g) of wurtzite ZnO structure can be calculated using Tauc's law [44]:

$$(\alpha h\nu)^2 = C^*(h\nu - E_g) \tag{1}$$

where, C^* is a constant, $h\nu$ is the photon energy and the α is the absorption coefficient calculated using [45]:

$$\alpha = (\frac{1}{d})\texttt{ln}(\frac{1}{T}) \tag{2}$$

Where, d is the thickness of the films and T is the transmittance. The optical band gap obtained by extrapolating the straight line portion to zero absorption coefficient ($\alpha = 0$) as shown in Fig. 6. Fig. 6 represents the Tauc's plot for samples annealed at 500 °C. The extracted E_g values of undoped ZnO, Sm and Ce doped ZnO and co-doped ZnO films were found to be 3.22, 3.16, 3.20 and 3.09 eV. The E_g values for the doped samples decreased compared undoped ZnO. A similar trend was previously observed for ZnO, Sm^{3+} and Al co-doped ZnO thin films prepared by the sol-gel method [23, 46, 47]. Moreover, the decrease in the band gap may be due to the formation of additional states below the conduction band caused the doping [48]. Generally, impurities can create energy levels in the band gap near the band edges. When the doping concentrations increased the density of the states of these dopants increases and form a continuum states, and as a result the band gap appears to decrease. Furthermore, this decrease in the energy gap could also be attributed to the band tailing. Bahşi and Oral [49] found that doping ZnO thin films with Mn and Cu increases the widths of the band tails due to a large number of transitions between the tails and bands (band to tails and tails to tails), which in turn causes red shift in the absorption edges and therefore decreases the band gap. Furthermore, the surface structure has also been reported as a reason behind the band gap reduction [22].
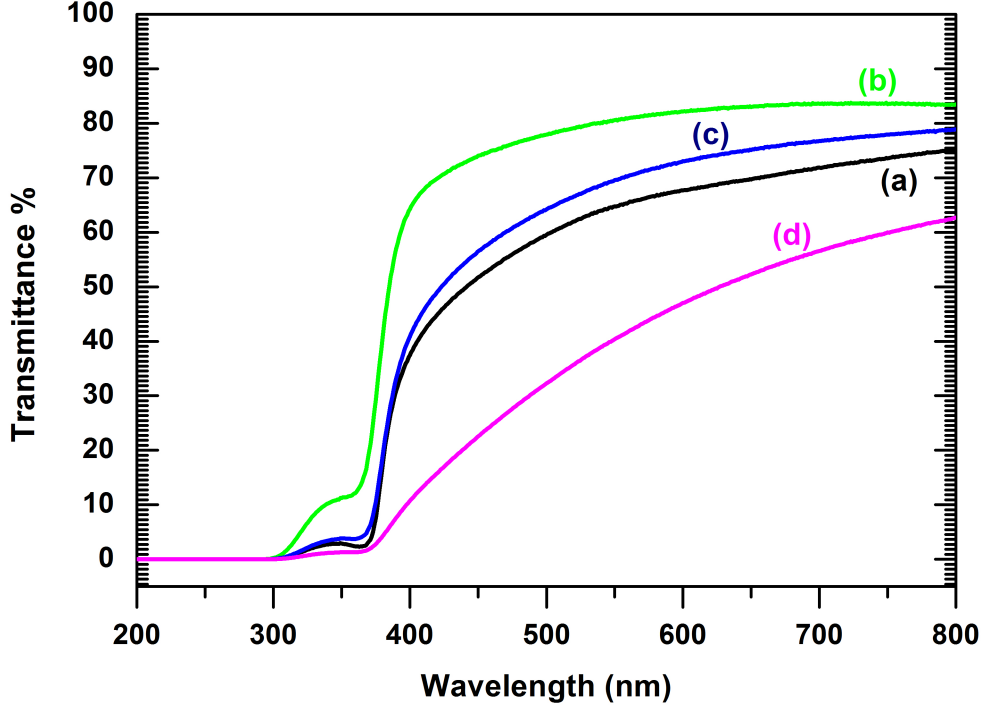
Figure 5: (Color online) Transmittance spectra of the samples annealed in air at 500 °C for 1 h: (a) undoped, (b) Sm-doped, (c) Ce-doped and (d) Sm and Ce co-doped ZnO thin films.

4.4. Current-voltage characteristic of Pd/ZnO/n$^+$-Si/AuSb Schottky diodes

Fig. 7 shows room temperature semilogarithmic *I-V* characteristics of Pd/ZnO/n$^+$-Si/AuSb Schottky diodes based on undoped, Sm and Ce doped ZnO and co-doped ZnO thin films, fabricated using sol-gel spin coating technique. As can be seen in Fig. 7 the structure exhibited rectification. The diode based on undoped ZnO showed rectification of two orders of magnitude. This result for undoped ZnO is similar to previously reported ZnO Schottky diodes prepared using sol-gel and spin coating [50]. As evidenced in Fig. 7, the maximum rectification obtained when ZnO is co-doped with Sm and Ce is almost six orders of magnitudes compared to undoped ZnO. However, the rectification ratio in the cases of Sm and Ce doped ZnO films are five and four orders of magnitude, respectively. The *I-V* characteristics of Schottky diodes without considering the series resistance can be described using the thermionic emission theory [51]:

$$I = I_s \left[1 - \exp\left(\frac{-q(V - IR_s)}{K_\beta T} \right) \right] \tag{3}$$

where, q is the electronic charge, R_s is the series resistance and I_s is the saturation current in the absence of external bias and it is given by:

$$I_s = S A^* T^2 [-q \frac{\Phi_{B_0}}{n K_\beta T}] \tag{4}$$

where, A^* is the effective Richardson constant, K_β is the Boltzmann constant, T is the absolute temperature, S is the diode contact area ($\approx 2.83 10^{-3}$ cm^2), Φ_{B_0} represents the zero bias Schottky barrier height, and the diode ideality factor denoted by n. The Schottky diode parameters, ideality factor n, Schottky barrier height Φ_{B0}, current saturation I_s and the series resistance R_s obtained from the fit using 3 and 4 are presented in Table 2.

As can be seen from Table. 2 the Φ_{B_0} increased from 0.66 to 0.76, 0.70 and 0.82 eV, whereas the ideality factor decreased from 2.84 to 2.83, 2.63 and 1.62, for samples 1, 2 3 and 4, respectively. The Φ_{B_0} for all samples obtained
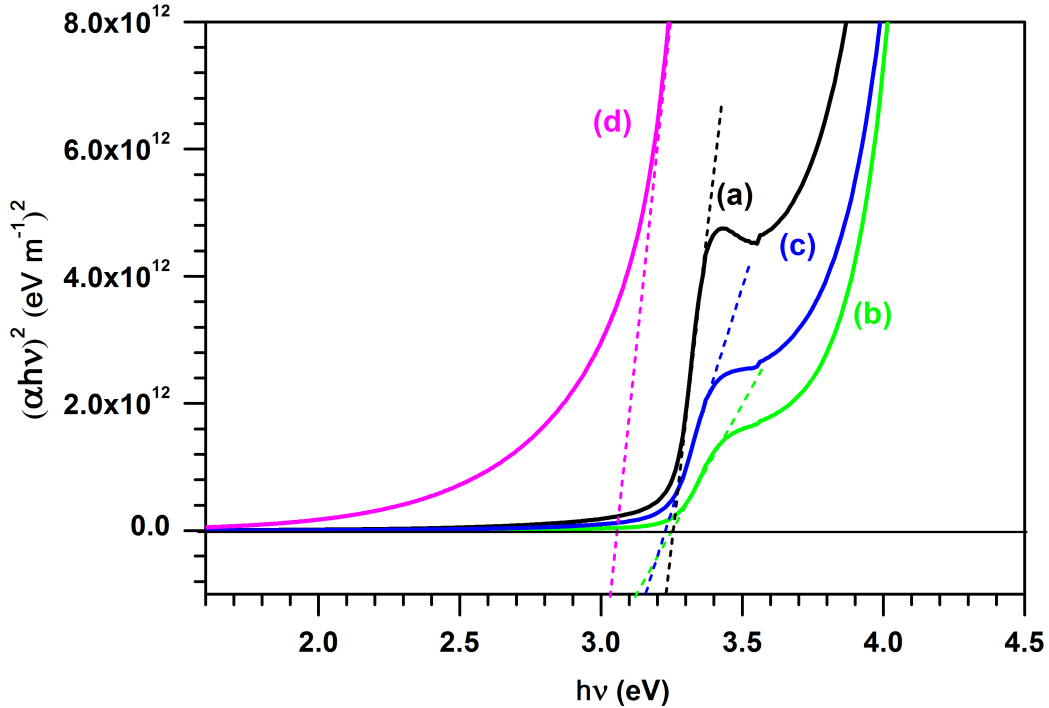
Figure 6: (Color online) Tauc's plot of samples annealed at 500 °C for 1 h : (a) undoped, (b) Sm-doped, (c) Ce-doped and (d) Sm and Ce co-doped ZnO thin films.

from the fit at zero applied voltage deviated from the theoretically calculated one by ∼ 1.00 eV (the difference between Pd work function and ZnO electron affinity). This deviation could be due to the presence of interface states, Schottky effect [8, 52], the formation of inhomogeneities in the barrier height at the interface which results as *I-V* characteristics deviate from linearity [53]. Moreover, thin films prepared using chemical methods in air have been shown to produce a dielectric layer that affects the barrier height [8]. The obtained *n* values for all samples were significantly above unity. This indicates that the behaviour of the Schottky diode is non-ideal (*n* = 1 for an ideal diode) and could be attributed to series resistance, interfacial charge distributions and voltage drops across the metal/semiconductor junction [54]. Obtained ideality factor for our Pure ZnO films is comparable with recently reported Si/ZnO heterojunction [55], and is in good agreement with *n* obtained for Pd Schottky diode on bulk ZnO single crystal [15]. After doping, *n* values for Sm and Ce doped ZnO thin films decreased compared to undoped ZnO and the values. The smallest value of *n* is obtained with Ce and Sm co-doped ZnO thin films. This result is much better than the value obtained for melt grown single crystal ZnO thin film [15]. This result also emphasizes that Sm and Ce co-doped ZnO thin films can be used as alternative Schottky diode.

The series resistance of the fabricated Schottky diodes showed the minimum value obtained for the Sm-doped ZnO sample. The largest value of the series resistance obtained for the undoped ZnO, where the deviation from the linearity is more pronounce (see Fig. 7 (a)). The lower series resistance could be attributed to the effect of the doping. From Fig. 7, it is observed that the best devices were obtained with Sm and Ce co-doping ZnO thin films. The lowest saturation current was obtained with Sm and Ce co-doped samples. Additionally, samples were also characterized after annealed in air instead of Ar and the *I-V* characteristics of these samples (not shown here) showed very high series resistance.

To understand the current transport mechanisms in our fabricated Schottky diodes, ln *I* vs ln *V* is plotted as shown in Fig. 8. As can be seen, three different regions: I, II and III are observed for undoped ZnO and (Sm, Ce) co-doped ZnO films which indicate three different mechanisms as shown in Fig. 8 (a) and (d). However, for the Sm and Ce
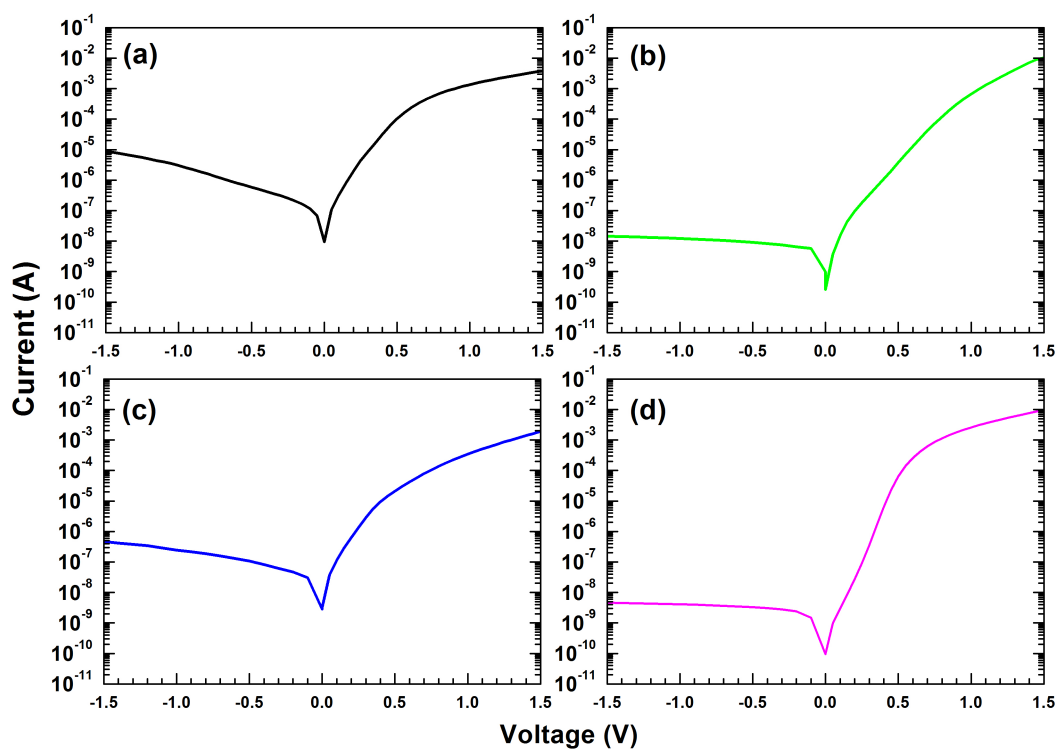
Figure 7: (Color online) Typical *I-V* characteristics of Pd/ZnO/n$^+$-Si/AuSb Schottky diodes annealed at 500 °C in argon: (a) undoped, (b) Sm-doped, (c) Ce-doped and (d) Sm and Ce co-doped ZnO thin films

Table 2: Schottky barrier height, ideality factor, saturation current and series resistance of Pd/ZnO/n$^+$-Si/AuSb Schottky diodes.

Samples	ϕ_{B0} (eV)	n	I_s (A)	$R_s(\Omega)$
1	0.66	2.84	1.14×10^{-7}	612
2	0.76	2.83	4.15×10^{-8}	29
3	0.70	2.63	2.67×10^{-8}	52
4	0.82	1.62	2.77×10^{-10}	60
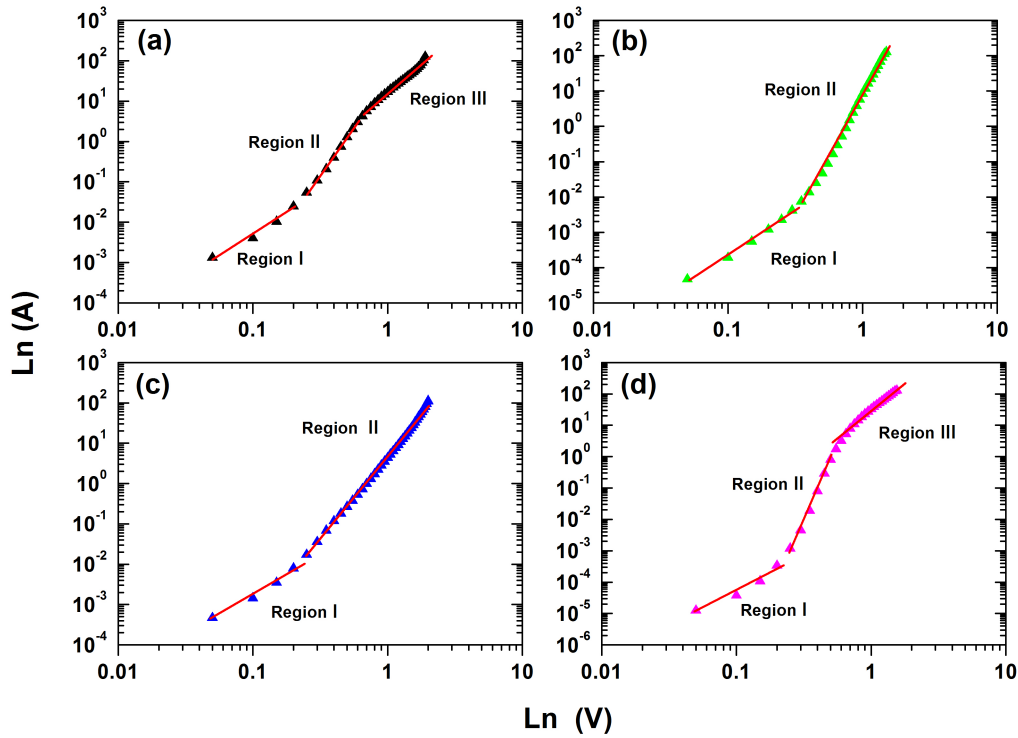
Figure 8: ln I vs ln V plots of the fabricated Schottky diode based on: (a) undoped ZnO, (b) Sm doped ZnO, (c) Ce doped ZnO and (d) is Sm and Ce co-doped ZnO thin films.

doped ZnO films only two regions: I and II are observed (see Fig. 8 (b) and (c)). It is clear that at lower voltage all Schottky diodes shows ohmic behaviour indicated by region I where the current is linearly dependent on the voltage ($I \sim V$), and the transport mechanism in this case attributed to the charge carriers tunneling between that states at the interface [56, 57]. In region II current is exponentially dependent on the voltage ($I \sim \exp(V)$) and the transport mechanism possibly attributed to the recombination tunneling [56]. Finally, in region III, the current shows power law dependency ($I \sim V^2$) and the transport mechanism is attributed to the space charge limited current (SCLC) due to the presence of traps at different energies within ZnO band gap [56, 57, 58].

5. Conclusion

In this study, we have successfully fabricated Pd/ZnO/n$^+$-Si/AuSb Schottky diodes based on undoped ZnO, Sm and Ce doped ZnO and co-doped ZnO thin films grown using the simple and low cost sol-gel spin coating technique. The structural, optical and electrical properties of the fabricated Schottky diodes were studied. XRD results revealed that the as-synthesized samples were polycrystalline with no other impurities or phases related to Sm or Ce detected,

indicating that the dopants have been incorporated successfully into the ZnO lattice structure. The PL spectra measured at room temperature revealed UV emission consisting of two peaks located at 388 nm and 405 nm. The PL spectra also revealed the absence of the deep level emission. UV-vis transmittance revealed that the optical band gap decreased when the dopnants introduced. Maximum transmittance (83 %) obtained when the ZnO was doped with Sm. The *I-V* characteristics of the fabricated Schottky diodes measured at room temperature manifest good rectification behaviour and the maximum (almost six orders of magnitude) was obtained with Sm and Ce co-doping ZnO. The (Sm, Ce) co-doped samples manifest a good device with the lowest ideality factor (1.62) and series resistance of 60 Ω. Furthermore, three different mechanisms are observed in our Schottky diodes; namely, the charge carries tunnelling, recombination tunnelling and space charge limited current.

Acknowledgment

References

[1] R. Bao, C. Wang, Z. Peng, C. Ma, L. Dong, C. Pan, Light-emission enhancement in a flexible and size-controllable ZnO nanowire/organic light-emitting diode array by the piezotronic effect, ACS Photonics 4 (6) (2017) 1344–1349.

[2] R. Vittal, K.-C. Ho, Zinc oxide based dye-sensitized solar cells: A review, Renew. Sust. Energ. Rev. 70 (2017) 920–935.

[3] A. Kogo, Y. Sanehira, Y. Numata, M. Ikegami, T. Miyasaka, Amorphous Metal Oxide Blocking Layers for Highly Efficient Low-Temperature Brookite TiO$_2$-Based Perovskite Solar Cells, ACS Appl. Mater. Interfaces 10 (3) (2018) 2224–2229.

[4] M. Ahmed, W. Meyer, J. Nel, Structural, optical and electrical properties of a Schottky diode fabricated on Ce doped ZnO nanorods grown using a two step chemical bath deposition, Mater. Sci. Semicond. Process. 87 (2018) 187–194.

[5] H. Kwon, J. H. Sung, Y. Lee, M.-H. Jo, J. K. Kim, Wavelength-dependent visible light response in vertically aligned nanohelical TiO$_2$-based Schottky diodes, Appl. Phys. Lett. 112 (4) (2018) 043106.

[6] V. Kabra, L. Aamir, M. Malik, Low cost, p-ZnO/n-Si , rectifying, nano heterojunction diode: Fabrication and electrical characterization, Beilstein J. Nanotechnol. 5 (2014) 2216.

[7] F. Tuomisto, K. Saarinen, D. C. Look, G. C. Farlow, Introduction and recovery of point defects in electron-irradiated ZnO, Phys. Rev. B. 72 (8) (2005) 085206.

[8] L. J. Brillson, Y. Lu, ZnO Schottky barriers and ohmic contacts, J. Appl. Phys. 109 (12) (2011) 8.

[9] D. C. Look, Recent advances in ZnO materials and devices, Mater. Sci. Eng. B 80 (1-3) (2001) 383–387.

[10] Y. L. Song, W. Jiang, P. F. Ji, Y. Li, F. Q. Zhou, N. Wen, A prototypical nanostructured ZnO/Si light-emitting diode based on the silicon nanoporous pillar array: Carriers transportation properties and white electroluminescence, J. Lumin. 192 (2017) 734–738.

[11] L. Rajan, C. Periasamy, V. Sahula, Comprehensive study on electrical and hydrogen gas sensing characteristics of Pt/ZnO nanocrystalline thin film-based Schottky diodes grown on n-Si substrate using RF sputtering, IEEE T. Nanotechnol. 15 (2) (2016) 201–208.

[12] S. Ameen, D. Park, M. Akhtar, H. Shin, Lotus-leaf like ZnO nanostructures based electrode for the fabrication of ethyl acetate chemical sensor, Mater. Lett. 164 (2016) 562–566.

[13] H. Liang, S. Yu, H. Yang, Directional and controllable edge-emitting ZnO ultraviolet random laser diodes, Appl. Phys. Lett. 96 (10) (2010) 101116.

[14] S. K. Singh, P. Hazra, S. Tripathi, P. Chakrabarti, Performance analysis of RF-sputtered ZnO/Si heterojunction UV photodetectors with high photo-responsivity, Superlattices Microstruct. 91 (2016) 62–69.

[15] W. Mtangi, F. D. Auret, C. Nyamhere, P. van Rensburg, A. Chawanda, M. Diale, J. M. Nel, W. E. Meyer, The dependence of barrier height on temperature for Pd Schottky contacts on ZnO, Physica B: Condens. Matter. 404 (22) (2009) 4402–4405.

[16] K. Ueda, H. Tabata, T. Kawai, Magnetic and electric properties of transition-metal-doped ZnO films, Appl. Phys. Lett. 79 (7) (2001) 988–990.

[17] M. S. Park, B. Min, Ferromagnetism in ZnO codoped with transition metals: Zn$_{1-x}$ (FeCo)$_x$ O and Zn$_{1-x}$ (FeCu)$_x$ O, Phys. Rev. B 68 (22) (2003) 224436.

[18] D. Sharma, R. Jha, Transition metal (Co, Mn) co-doped ZnO nanoparticles: effect on structural and optical properties, J. Alloys Compd. 698 (2017) 532–538.

[19] N. Fifere, A. Airinei, D. Timpu, A. Rotaru, L. Sacarescu, L. Ursu, New insights into structural and magnetic properties of Ce doped ZnO nanoparticles, J. Alloys Compd. 757 (2018) 60–69.

[20] E. Asikuzun, O. Ozturk, L. Arda, A. Tasci, F. Kartal, C. Terzioglu, High-quality c-axis oriented non-vacuum Er doped ZnO thin films, Ceram. Int. 42 (7) (2016) 8085–8091.

[21] R. Kumar, A. Umar, G. Kumar, M. Akhtar, Y. Wang, S. Kim, Ce-doped ZnO nanoparticles for efficient photocatalytic degradation of direct red-23 dye, Ceram. Int. 41 (6) (2015) 7773–7782.

[22] R. Zamiri, A. Lemos, A. Reblo, H. A. Ahangar, J. Ferreira, Effects of rare-earth (Er, La and Yb) doping on morphology and structure properties of ZnO nanostructures prepared by wet chemical method, Ceram. Int. 40 (1) (2014) 523–529.

[23] V. Anand, A. Sakthivelu, K. D. Kumar, S. Valanarasu, A. Kathalingam, V. Ganesh, M. Shkir, S. AlFaify, I. Yahia, Rare earth Sm^{3+} co-doped AZO thin films for opto-electronic application prepared by spray pyrolysis, Ceram. Int. 44 (6) (2018) 6730–6738.

[24] A. J. Kulandaisamy, V. Elavalagan, P. Shankar, G. K. Mani, K. J. Babu, J. B. B. Rayappan, Nanostructured cerium-doped ZnO thin film–A breath sensor, Ceram. Int. 42 (16) (2016) 18289–18295.

[25] Y. Xiang, Z. Ma, J. Zhuang, H. Lu, C. Jia, J. Luo, H. Li, X. Cheng, Enhanced Performance for Planar Perovskite Solar Cells with Samarium-Doped TiO$_2$ Compact Electron Transport Layers, J. Phys. Chem. C 121 (37) (2017) 20150–20157.

[26] M. A. M. Ahmed, B. S. Mwankemwa, E. Carleschi, B. P. Doyle, W. E. Meyer, J. M. Nel, Effect of Sm doping ZnO nanorods on structural optical and electrical properties of Schottky diodes prepared by chemical bath deposition, Mater. Sci. Semicond. Process. 79 (8) (2018) 53 – 60.

[27] D. C. Look, D. Reynolds, C. Litton, R. Jones, D. Eason, G. Cantwell, Characterization of homoepitaxial p-type ZnO grown by molecular beam epitaxy, Appl. phys. lett. 81 (10) (2002) 1830–1832.

[28] J. Y. Park, D. J. L, S. S. Kim, Size control of ZnO nanorod arrays grown by metalorganic chemical vapour deposition, Nanotechnol. 16 (10) (2005) 2044.

[29] K. Reddy, H. Gopalaswamy, P. Reddy, R. Miles, Effect of gallium incorporation on the physical properties of ZnO films grown by spray pyrolysis, J. Cryst. Growth 210 (4) (2000) 516–520.

[30] B. Jin, S. Im, S. Y. Lee, Violet and UV luminescence emitted from ZnO thin films grown on sapphire by pulsed laser deposition, Thin Solid Films 366 (1-2) (2000) 107–110.

[31] A. Zak, N. Aziz, A. M. Hashim, F. Kordi, XPS and UV–vis studies of Ga-doped zinc oxide nanoparticles synthesized by gelatin based sol-gel approach, Ceram. Int. 42 (12) (2016) 13605–13611.

[32] A. Farag, W. Farooq, F. Yakuphanoglu, Characterization and performance of Schottky diode based on wide band gap semiconductor ZnO using a low-cost and simplified sol–gel spin coating technique, Microelectron. Eng. 88 (9) (2011) 2894–2899.

[33] L. Znaidi, T. Chauveau, A. Tallaire, F. Liu, M. Rahmani, V. Bockelee, D. Vrel, P. Doppelt, Textured ZnO thin films by sol–gel process: Synthesis and characterizations, Thin Solid Films 617 (2016) 156–160.

[34] G. Murtaza, M. A. Iqbal, Y. B. Xu, I. G. Will, Z. C. Huang, Study of Sm-doped ZnO samples sintered in a nitrogen atmosphere and deposited on n-si (1 0 0) by evaporation technique, J. Mag. Magn. Mater. 323 (24) (2011) 3239–3245.

[35] U. Holzwarth, N. Gibson, The scherrer equation versus the'Debye-Scherrer equation', Nat. Nanotechnol. 6 (9) (2011) 534–534.

[36] M. Yousefi, M. Amiri, R. Azimirad, A. Z. Moshfegh, Enhanced photoelectrochemical activity of Ce doped ZnO nanocomposite thin films under visible light, J. Electroanal Chem. 661 (1) (2011) 106–112.

[37] D. Bagnall, Y. Chen, Z. Zhu, T. Yao, S. Koyama, M. Y. Shen, T. Goto, Optically pumped lasing of ZnO at room temperature, Appl. Phys. Lett. 70 (17) (1997) 2230–2232.

[38] W. I. Park, Y. H. Jun, S. W. Jung, G. Yi, Excitonic emissions observed in ZnO single crystal nanorods, Appl. Phys. Lett. 82 (6) (2003) 964–966.

[39] B. Djurišić, Y. Leung, Optical properties of ZnO nanostructures, Small 2 (8-9) (2006) 944–961.

[40] C. Singh, E. Panda, Variation of electrical properties in thickening Al-doped ZnO films: Role of defect chemistry, RSC Adv. 6 (54) (2016) 48910–48918.

[41] A. B. Djurišić, W. Choy, V. A. L. Roy, Y. H. Leung, C. Y. Kwong, K. W. Cheah, T. Gundu Rao, W. K. Chan, H. Fei Lui, C. Surya, Photoluminescence and electron paramagnetic resonance of ZnO tetrapod structures, Adv. Func. Mater. 14 (9) (2004) 856–864.

[42] M. Wang, K. E. Lee, S. H. Hahn, E. J. Kim, S. Kim, J. S. Chung, E. W. Shin, C. Park, Optical and photoluminescent properties of sol-gel Al-doped ZnO thin films, Mater. Lett. 61 (4-5) (2007) 1118–1121.

[43] A. M. Torres-Huerta, M. Dominguez-Crespo, S. Brachetti-Sibaja, H. Dorantes-Rosales, M. Hernandez-Perez, J. Lois-Correa, Preparation of ZnO: CeO$_{2-x}$ thin films by AP-MOCVD: Structural and optical properties, J. Solid State Chem. 183 (9) (2010) 2205–2217.

[44] Z. Wu, J. Cai, G. Ni, ZnO films fabricated by chemical bath deposition from zinc nitrate and ammonium citrate tribasic solution, Thin Solid Films 516 (21) (2008) 7318–7322.

[45] J. Chen, D. Chen, J. He, S. Zhang, Z. Chen, The microstructure, optical, and electrical properties of sol-gel-derived Sc-doped and Al-Sc co-doped ZnO thin films, Appl. Surf. Sci. 255 (23) (2009) 9413–9419.

[46] N. Kamarulzaman, M. F. Kasim, R. Rusdi, Band gap narrowing and widening of ZnO nanostructures and doped materials, Nanoscale Res Lett. 10 (1) (2015) 346.

[47] A. Chelouche, T. Touam, M. Tazerout, F. Boudjouan, D. Djouadi, A. Doghmane, Low cerium doping investigation on structural and photoluminescence properties of sol-gel ZnO thin films, Journal of Luminescence 181 (2017) 448–454.

[48] S. Palimar, K. V. Bangera, G. Shivakumar, Highly conducting and transparent Ga$_2$O$_3$ doped ZnO thin films prepared by thermal evaporation method, Semiconductors 46 (12) (2012) 1545–1548.

[49] Z. B. Bahşi, A. Y. Oral, Effects of Mn and Cu doping on the microstructures and optical properties of sol–gel derived ZnO thin films, Opt. Mater. 29 (6) (2007) 672–678.

[50] F. Yakuphanoglu, Electrical characterization and device characterization of ZnO microring shaped films by sol–gel method, J. Alloys Compd 507 (1) (2010) 184–189.

[51] E. Rhoderick, R. Williams, M.-S. Contacts, 2nd edn, Clarendon, Oxford.

[52] H. Von Wenckstern, E. Kaidashev, M. Lorenz, H. Hochmuth, G. Biehne, J. Lenzner, V. Gottschalch, R. Pickenhain, M. Grundmann, Lateral homogeneity of Schottky contacts on n-type ZnO, Appl. Phys. lett. 84 (1) (2004) 79–81.

[53] D. Korucu, T. Mammadov, Temperature-dependent current-conduction mechanisms in Au/n-InP Schottky barrier diodes (SBDs), J. Opto-electron. Adv. Mater. 14 (1) (2012) 41.

[54] N. Singh, L. Kumar, A. Kumar, S. Vaisakh, S. Singh, K. Sisodiya, S. Srivastava, M. Kansal, S. Rawat, T. Singh, et al., Fabrication of zinc oxide/polyaniline (ZnO/PANI) heterojunction and its characterisation at room temperature, Mater. Sci. Semicond. Process. 60 (2017) 29–33.

[55] S. K. S, P. H, Analysis of current transport mechanisms in sol-gel grown Si/ZnO heterojunction diodes in high temperature environment, Superlattice. Microst. 128 (2019) 48–55.

[56] J. Hwang, C. Kung, Y. Lin, Non-surface-treated Au/ZnO Schottky diodes using pre-annealed hydrothermal or sol-gel seed layer, IEEE Trans.

Nanotechnol. 12 (1) (2013) 35–39.

[57] D. Somvanshi, S. Jit, Effects of Sn and Zn Seed Layers on the Electrical characteristics of Pd/ZnO thin-film Schottky Diodes Grown on n-Si Substrates, IEEE Electron Device Lett. 35 (9) (2014) 945–947.

[58] Ş. Aydoğan, K. Çınar, H. Asıl, C. Coşkun, A. Türüt, Electrical characterization of Au/n-ZnOSchottky contacts on n-Si, J. Alloy. Compd. 476 (1-2) (2009) 913–918.